J. Phys.: Condens. Matter **10** (1998) 9015–9027. Printed in the UK PII: S0953-8984(98)92395-5

Charging effects in the alternating-current conductance of a double-barrier resonant tunnelling structure

M P Anantram

NASA Ames Research Center, Mail Stop: T27-A, Moffett Field, CA 94035-1000, USA

Received 10 March 1998, in final form 17 June 1998

Abstract. There have been many studies of the linear response ac conductance of a double-barrier resonant tunnelling structure. While these studies are important, they fail to self-consistently include the effect of time-dependent charge density in the well. In this paper, we calculate the ac conductance by including the effect of time-dependent charge density in the well in a self-consistent manner. The charge density in the well contributes to both the flow of displacement currents and the time-dependent potential in the well. We find that including these effects can make a significant difference to the ac conductance, and that the total ac current is not equal to the average of non-self-consistently calculated conduction currents in the two contacts, an assumption often made. This is illustrated by comparing the results obtained with and without the effect of the time-dependent charge density included properly.

1. Introduction

Double-barrier resonant tunnelling structures (DBRTS) have been of great interest because of possible device applications in building logic circuits, oscillators, detectors etc, and they have much to offer in the study of the physics of confined structures. The dc characteristics have been studied extensively by including the effects of charging and inelastic scattering. Reference [1] offers a comprehensive review of applications and the basic physics of DBRTS. In contrast, there are only a few studies of the ac response over various frequency regimes [2–7]. While some of these studies are based on simulating a realistic device using detailed numerical procedures [2, 3], others are based on simple models [4–7]. These calculations however do not include the effect of time-varying charge density in the well, which is important in determining ac conductance [3, 4, 8–10]. While reference [8] has discussed the pitfalls of many existing ac conductance theories qualitatively, reference [9] formulated the theory of ac conductance in the linear response and low-frequency regime as applicable to mesoscopic structures by including the effects of charging. Subsequently, reference [12] used a non-equilibrium Green's function approach to provide a formulation that can be used at finite biases and large frequencies including effects of charging in the well and phonon scattering [13]. The effect of time-dependent charge density in the well is of importance in determining the dynamics, because electrons in the well image to the outside world, which includes the contacts. This causes the flow of displacement currents and contributes to the ac potential in the well. The role of these factors in determining the ac conductance of a DBRTS is not clear from previous work. In this paper, we study the ac conductance of a DBRTS with the aim of illustrating the role of imaging of well charge to contacts via a simple model. Imaging of well charge to the two contacts is modelled by capacitances denoted by C_1 and C_2 (figure 1). We would like to clarify at the outset

0953-8984/98/409015+13$19.50

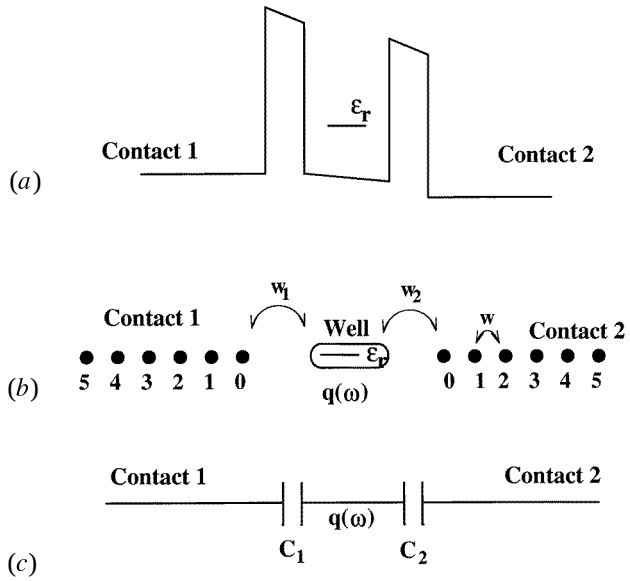

Figure 1. (a) The band structure of a DBRTS. (b) The DBRTS is modelled by the tight-binding Hamiltonian. (c) Imaging of charge from the well to the contacts is accounted for by capacitive coupling between the well and the contacts via capacitances C_1 and C_2.

that the purpose of this study is to illustrate the importance of imaging and not to model a typical resonant tunnelling device, whose structure is considerably more complicated.

We derive useful expressions for the ac conductance and show that the ac conductance depends significantly on both (i) the ratio of capacitances C_1/C and C_2/C, where $C = C_1 + C_2$, and (ii) the value of the total capacitance between the well and the contacts. The first feature follows because a time-dependent well charge $q(t)$ contributes to a flow of displacement currents equal to

$$\frac{C_1}{C}\frac{\mathrm{d}q(t)}{\mathrm{d}t} \qquad \text{and} \qquad \frac{C_2}{C}\frac{\mathrm{d}q(t)}{\mathrm{d}t}$$

in contacts 1 and 2 respectively (figure 1), where $q(t)$ is the charge in the well at time t. The second feature can be understood by noting that the time-dependent charge density in the well contributes to ac potential of the well via a term $q(t)/C$ (figure 1). This affects the current because the ac potential in the well plays a role in determining both the conduction and displacement currents. Note that there is nothing quantum mechanical about these two features, and they would still arise even if C_1 and C_2 were leaky capacitors in a classical circuit. Quantum mechanics plays a role only in determining the values of $q(t)$ and the current.

Some previous papers calculated the ac conductance of a DBRTS by the following procedure (see section 3). The conduction currents across the two barriers are calculated by neglecting the contribution to the ac potential in the well from the time-dependent charge density. Then the total ac current is taken to be the average of the conduction currents flowing across the two barriers. *We find such a procedure to be valid only when the capacitances are symmetrical ($C_1 = C_2$) and the value of C is large.*

The remainder of the paper is arranged as follows. In section 2, we have explained the model adopted in detail. In section 3, we discuss the effect of charging on the ac conductance

using expressions derived in section 2.2. In section 4, we discuss the effect of charging on the ac conductance using numerical examples. The effect of including asymmetries in the barrier strengths and the capacitances of an otherwise symmetric structure are systematically studied here. We present our conclusions in section 5.

2. The model

2.1. The Hamiltonian

We model the resonant tunnelling structure using a tight-binding Hamiltonian [4–7, 14, 15]. The well is represented by a single node with a resonant level at energy ϵ_r and is coupled to contacts 1 and 2 (figure 1). The Hamiltonian of the structure is

$$H = H_D + H_C + H_{CD} \tag{2.1}$$

where

$$H_D = \epsilon_r(t) d^\dagger d$$
$$H_C = \sum_{i,\alpha \in 1,2} (\epsilon_{i\alpha} + e v_1^{ac} \cos(\omega t)\delta_{1,\alpha}) c_{i\alpha}^\dagger c_{i\alpha} + (w c_{i\alpha}^\dagger c_{i+1\alpha} + \text{C·C})$$
$$H_{CD} = \sum_{\alpha \in 1,2} w_\alpha c_{0\alpha}^\dagger d + \text{C·C.}$$

We assume that the ac potential is applied only to contact 1. d ($d^\dagger$) and $c_{i\alpha}$ ($c_{i\alpha}^\dagger$) are annihilation (creation) operators for electrons in the well and various lattice sites of contact α respectively. The sites in a contact are labelled starting from 0 which represents the lattice site immediately neighbouring the well. w_1 and w_2 represent the coupling between the well and site 0 of contacts 1 and 2 respectively. w represents the coupling between nearest neighbours in the tight-binding lattice of the contacts. H_D, H_C and H_{CD} represent the Hamiltonians of the isolated well, contacts and coupling between the well and contacts respectively. In the presence of a dc bias V_α^{dc} applied to contact α, the on-site potential in contact α increases by the dc bias ($\epsilon_{i\alpha} \to \epsilon_{i\alpha} + eV_\alpha^{dc}$). The expression for $\epsilon_r(t)$ is

$$\epsilon_r(t) = \epsilon_{r0} + \beta_2 e V_{dc} + \alpha_2 e v_1^{ac}(t) + e V_w^Q(t) \tag{2.2}$$

where ϵ_{r0} is the energy of the resonant level at zero dc and ac biases. V_{dc} and v_1^{ac} are dc and ac biases applied to contact 1. β_2 and α_2 are fractional drops of the external dc and ac potentials between contact 2 and the well respectively, in the absence of charge in the well. The last term of equation (2.2) represents the effect of imaging of charge in the well. The electrons in the well image to the contacts and this is modelled by capacitances C_1 and C_2 (figure 1), which are assumed to be known parameters [9, 14]. As a consequence of imaging of the well charge, the band bottom in the well (and hence the resonant level) changes by $V_w^Q(t)$:

$$V_w^Q(t) = \frac{q(t)}{C} = V_w^{dc} + v_w^{ac}(t) \tag{2.3}$$

where

$$V_w^{dc} = \frac{q_{dc}(V)}{C} \qquad \text{and} \qquad v_w^{ac}(t) = \frac{q(t) - q_{dc}(V)}{C}. \tag{2.4}$$

$q_{dc}(V)$ represents the dc charge in the well when the applied dc voltage is V. $q(t)$ is the total charge in the well and $q(t) - q_{dc}(V)$ is the time-dependent component. The total capacitance between the well and contacts is C ($=C_1 + C_2$).

The total potential in the well, $V_w(t)$, is

$$V_w(t) = V_w^Q(t) + \beta_2 V_{dc} + \alpha_2 v_1^{ac}(t). \tag{2.5}$$

The first, second and third terms represent the potentials due to imaging of the well charge, the externally applied dc and ac potentials respectively.

2.2. ac conductance

The applied ac voltage results in a time-dependent well charge that images to the contacts. This (i) causes a flow of displacement currents and (ii) contributes to the time-dependent potential of the well (V_w^Q of equation (2.3)). (ii) plays a role in determining the correct conduction currents. The conduction current is in turn related to the time-varying well charge by a continuity equation (equation (2.10)).

In the following discussion, we first define a conductance matrix, **g**. The conduction and displacement currents are then expressed in terms of the elements of the conductance matrix. The procedure for evaluating the conductance matrix is discussed in the next subsection.

*2.2.1. The conductance matrix (**g**).* The conductance matrix element $g_{\alpha\beta}$ represents the ratio of the conduction current (i_α^c) flowing in contact α as a result of an ac voltage (v_β) applied to contact β, with the ac potential in the well and contacts set equal to zero:

$$g_{\alpha\beta}(\omega) = \frac{i_\alpha^c(\omega)}{v_\beta^{ac}(\omega)} \qquad \text{where } \alpha, \beta \in 1, 2. \tag{2.6}$$

The dc voltage is set to its steady-state value, i.e., the dc component of equation (2.5).

2.2.2. The conduction current. Consider an ac potential v_1^{ac} applied to contact 1, with contact 2 grounded. As a result, the potential of the well develops a time-dependent component, $v_w(\omega)$ (equation (2.5) [16]). The linear response ac current flowing in contact $i \in 1, 2$ consists of two terms, (i) due to the ac potential v_1^{ac}, with the ac potentials in the well and contact 2 set equal to zero, and (ii) due to the ac potential $v_w(\omega)$ in the well, with the ac potential in contacts 1 and 2 set equal to zero. The first component is $g_{i1}v_1^{ac}$. This follows from the definition in equation (2.6). The second component is physically equivalent to setting the ac potential in the well equal to zero along with an ac potential $-v_w(\omega)$ applied to contacts 1 and 2. The linear response current flowing in contact i due to this component is $-(g_{i1} + g_{i2})v_w(\omega)$ (from equation (2.6)). The total ac conduction current flowing in contacts 1 and 2 is the sum of the two components:

$$\begin{aligned} &\text{ac conduction current in contact } 1 = g_{11}(\omega)(v_1^{ac}(\omega) - v_w(\omega)) + g_{12}(\omega)(-v_w(\omega)) \\ &\text{ac conduction current in contact } 2 = g_{21}(\omega)(v_1^{ac}(\omega) - v_w(\omega)) + g_{22}(\omega)(-v_w(\omega)). \end{aligned} \tag{2.7}$$

Now, if external ac potentials $v_1^{ac}(\omega)$ and $v_2^{ac}(\omega)$ are applied to both contacts 1 and 2, then the conduction current in the two contacts is given by

$$I_1^c(\omega) = g_{11}(\omega)(v_1^{ac}(\omega) - v_w(\omega)) + g_{12}(\omega)(v_2^{ac}(\omega) - v_w(\omega)) \tag{2.8}$$

$$I_2^c(\omega) = g_{21}(\omega)(v_1^{ac}(\omega) - v_w(\omega)) + g_{22}(\omega)(v_2^{ac}(\omega) - v_w(\omega)). \tag{2.9}$$

The well charge is related to the conduction currents by the continuity equation:

$$\frac{\mathrm{d}q(t)}{\mathrm{d}t} = I_1^c(t) + I_2^c(t) \rightarrow q(\omega) = \frac{I_1^c(\omega) + I_2^c(\omega)}{-\mathrm{i}\omega}. \tag{2.10}$$

Substituting equation (2.10) in equation (2.3) and equation (2.5), the ac potential of the device can be written as

$$v_w(\omega) = \alpha_2 v_1^{ac}(\omega) + \frac{I_1^c(\omega) + I_2^c(\omega)}{-\mathrm{i}\omega C}. \tag{2.11}$$

Using equations (2.8), (2.9) and (2.11), the conduction currents in contacts 1 and 2 can be expressed in terms of the g-matrix elements:

$$G_1^c(\omega) = \frac{I_1^c(\omega)}{v_1^{ac}} = +\frac{\alpha_1 g_{11} - \alpha_2 g_{12} + (1/[-\mathrm{i}\omega C])(g_{11}g_{22} - g_{12}g_{21})}{1 + (1/[-\mathrm{i}\omega C])(g_{11} + g_{22} + g_{12} + g_{21})} \tag{2.12}$$

$$G_2^c(\omega) = \frac{I_2^c(\omega)}{v_1^{ac}} = -\frac{\alpha_2 g_{22} - \alpha_1 g_{21} + (1/[-\mathrm{i}\omega C])(g_{11}g_{22} - g_{12}g_{21})}{1 + (1/[-\mathrm{i}\omega C])(g_{11} + g_{22} + g_{12} + g_{21})}. \tag{2.13}$$

Here α_1 and α_2 are fractional drops in the externally applied ac potential between the well and contacts 1 and 2 respectively, in the absence of charge in the well.

2.2.3. The displacement current. The displacement current flowing in contact α consists of two components. One component, $\pm\mathrm{i}\omega C$ (the plus and minus signs are for the currents in the two different contacts), is due to the dielectric nature of the barrier and well. This component does not depend on tunnelling of charge from the contacts to the well and is not explicitly written in the remainder of the paper. The other component, which is due to tunnelling of charge from the contacts to the well, is equal to $\mathrm{i}\omega C_\alpha/C$. The total displacement currents in the two contacts are given by

$$I_1^d(\omega) = \mathrm{i}\omega\frac{C_1}{C}q(\omega) = -\frac{C_1}{C}(I_1^c(\omega) + I_2^c(\omega)) \tag{2.14}$$

$$I_2^d(\omega) = \mathrm{i}\omega\frac{C_2}{C}q(\omega) = -\frac{C_2}{C}(I_1^c(\omega) + I_2^c(\omega)). \tag{2.15}$$

Solving equations (2.8)–(2.15), we get the following expression for the conductance contributions from the conduction and displacement currents:

$$G_\alpha^d(\omega) = \frac{I_\alpha^d(\omega)}{v_1^{ac}} = \frac{C_\alpha}{C}\frac{\alpha_1(g_{11} + g_{21}) - \alpha_2(g_{22} + g_{12})}{1 + (1/[-\mathrm{i}\omega C])(g_{11} + g_{22} + g_{12} + g_{21})} \tag{2.16}$$

where, $\alpha = 1, 2$ and ω has been suppressed in the arguments of the g-matrix elements.

2.2.4. The total current. Using equations (2.14) and (2.15), it can be seen that the total current (conduction plus displacement) in the contacts can be expressed in terms of the conduction currents:

$$I_1(\omega) = I_1^c(\omega) + I_1^d(\omega) = \frac{C_2}{C}I_1^c(\omega) - \frac{C_1}{C}I_2^c(\omega) \tag{2.17}$$

and

$$I_2(\omega) = I_2^c(\omega) + I_2^d(\omega) = \frac{C_1}{C}I_2^c(\omega) - \frac{C_2}{C}I_1^c(\omega) = -I_1(\omega). \tag{2.18}$$

We would like to emphasize that $I_1^c(\omega)$ and $I_2^c(\omega)$ are the conduction currents calculated by including the contribution to the ac potential in the well due to the ac well charge density. In the remainder of the paper it is assumed that α_1 and α_2 are equal to fractional drops in the potentials across C_1 and C_2 (figure 1). Then, $\alpha_1 = C_2/C$ and $\alpha_2 = C_1/C$. Substituting equations (2.12) and (2.13) in equations (2.17) and (2.18), the total ac conductance is

$$G_1(\omega) = +\frac{{\alpha_1}^2 g_{11} + {\alpha_2}^2 g_{22} - \alpha_2\alpha_1(g_{12} + g_{21}) + (1/[-\mathrm{i}\omega C])(g_{11}g_{22} - g_{12}g_{21})}{1 + (1/[-\mathrm{i}\omega C])(g_{11} + g_{22} + g_{12} + g_{21})} \tag{2.19}$$

$$G_2(\omega) = -G_1(\omega). \tag{2.20}$$

2.3. Calculation of the conductance matrix elements: $g_{\alpha\beta}$

The general expression for the ac conduction current in contact α taken from reference [12] is

$$i_\alpha(\omega) = \frac{e}{\hbar}\int_{-\infty}^{+\infty}\frac{\mathrm{d}E}{2\pi}\ \mathrm{Tr}\{i_\alpha^{(1)}(E,\omega) + i_\alpha^{(2)}(E,\omega) + i_\alpha^{(3)}(E,\omega) + i_\alpha^{(4)}(E,\omega)\} \tag{2.21}$$

where

$$i_\alpha^{(1)}(E,\omega) = \sigma_\alpha^<(E+\hbar\omega,E)[G^r(E+\hbar\omega) - G^a(E)] \tag{2.22}$$

$$i_\alpha^{(2)}(E,\omega) = -\mathrm{i}\Gamma_\alpha g^<(E+\hbar\omega,E) \tag{2.23}$$

$$i_\alpha^{(3)}(E,\omega) = g^r(E+\hbar\omega,E)\Sigma_\alpha^<(E) - g^a(E+\hbar\omega,E)\Sigma_\alpha^<(E+\hbar\omega) \tag{2.24}$$

$$i_\alpha^{(4)}(E,\omega) = \sigma_\alpha^r(E+\hbar\omega,E)G^<(E) - G^<(E+\hbar\omega)\sigma^a(E+\hbar\omega,E). \tag{2.25}$$

Here the functions represented by capital letters are calculated in the steady-state limit and the functions represented by lower-case letters are calculated to first order in the applied ac potential. G^r, g^r, G^a and g^a are retarded and advanced Green's functions at the site representing the well. Similarly, Σ_α^r, σ_α^r, Σ_α^a and σ_α^a are retarded and advanced self-energies at the well site due to coupling with contact α. The function $\Sigma_\alpha^<(E)$ represents the injection of electrons from contact α to the device at energy E. $\sigma_\alpha^<(E+\hbar\omega,E)$ represents the time-dependent injection from contact α to the device.

Using the expressions for dc [15, 17] and ac [12] self-energies, applying an ac potential to contact β yields

$$\Sigma_\alpha^r(E) = \mathrm{i}\Gamma_\alpha(E) \tag{2.26}$$

$$\Sigma_\alpha^<(E) = \mathrm{i}\Gamma_\alpha(E)f_\alpha(E) \tag{2.27}$$

$$\sigma_\alpha^r(E+\omega,E) = \frac{\Sigma_\alpha^r(E) - \Sigma_\alpha^r(E+\omega)}{\omega}\delta_{\alpha\beta} \tag{2.28}$$

$$\sigma_\alpha^<(E+\omega,E) = \frac{\Sigma_\alpha^<(E) - \Sigma_\alpha^<(E+\omega)}{\omega}\delta_{\alpha\beta} \tag{2.29}$$

where, α stands for contacts 1 and 2. In the expression for the retarded self-energy, we only keep the imaginary part and neglect the real part which represents a shift in the resonant energy [17].

In the dc limit the expression for $\Gamma_\alpha(E)$ is [18]

$$\Gamma_\alpha(E) = \frac{w_\alpha^2}{w}\sin(k_\alpha a) \qquad \text{for } E > V_\alpha \tag{2.30}$$

$$\Gamma_\alpha(E) = 0 \qquad \text{for } E < V_\alpha. \tag{2.31}$$

Due to the absence of inter-mode scattering, the Green's functions take the following form using expressions for g and G from [12] and [15] respectively:

$$G^r(E) = \frac{1}{E - \epsilon_{r0} + \Sigma(E)} \tag{2.32}$$

$$G^<(E) = G^r(E)\Sigma^<(E)G^a(E) \tag{2.33}$$

$$g^r(E+\omega,E) = G^r(E+\omega)\sigma^r(E+\omega,E)G^r(E) \tag{2.34}$$

$$\begin{aligned} g^<(E+\omega,E) = {} & G^r(E+\omega)\sigma^<(E+\omega,E)G^a(E) + g^r(E+\omega,E)\Sigma^<(E)G^a(E) \\ & + G^r(E+\omega)\Sigma^<(E+\omega)g^a(E+\omega,E)\}. \end{aligned} \tag{2.35}$$

Using equations (2.26)–(2.29) and equations (2.32)–(2.35) in equation (2.21), the various conductance matrix elements are calculated.

3. The effect of charging on the ac current

Many references calculate the ac current by neglecting the effect of charging in the device [2–7]. Specifically, reference [6] calculates the ac conduction currents flowing in the two contacts by neglecting the effect of charging. It is then asserted that the total ac current is equal to the average of the calculated conduction currents in the two contacts:

$$I(\omega) = \frac{1}{2}(i_1^c(\omega) - i_2^c(\omega)) \tag{3.1}$$

where, $i_1^c(\omega)$ and $i_2^c(\omega)$ are conduction currents calculated by neglecting charging.

To illustrate the importance of charging and to show that equation (3.1) is valid only under special circumstances, we summarize our line of argument from the previous section.

The total current is the sum of the conduction and displacement currents:

$$I_1(\omega) = I_1^c(\omega) + I_1^d(\omega) \qquad \text{and} \qquad I_2(\omega) = I_2^c(\omega) + I_2^d(\omega).$$

The conduction currents here should be calculated by including the effect of the potential in the well due to the time-varying charge density in the well (equation (2.3)). The displacement currents are related to the time-dependent charge density and are given by

$$I_1^d(\omega) = \mathrm{i}\omega\frac{C_1}{C}q(\omega) \qquad \text{and} \qquad I_2^d(\omega) = \mathrm{i}\omega\frac{C_2}{C}q(\omega).$$

Now $q(\omega)$ in the above equations can be related to the conduction currents using the continuity equation:

$$\frac{\mathrm{d}q(t)}{\mathrm{d}t} = I_1^c(t) + I_2^c(t) \longrightarrow q(\omega) = \frac{I_1^c(\omega) + I_2^c(\omega)}{-\mathrm{i}\omega}.$$

Using the last five equations, the total current can be expressed in terms of the conduction currents (calculated by including the effect of charging in the well) as

$$I_1(\omega) = \frac{C_2}{C}I_1^c(\omega) - \frac{C_1}{C}I_2^c(\omega) \qquad \text{and} \qquad I_2(\omega) = \frac{C_1}{C}I_2^c(\omega) - \frac{C_2}{C}I_1^c(\omega).$$

From these equations, we see that equation (3.1) is an appropriate expression for the conduction current only when both $C_1 = C_2$ and the conduction currents are calculated by neglecting the effect of charging.

In terms of our notation involving the g-matrix elements, equation (3.1) corresponds to the following equation which is obtained by setting $C = \infty$ and $C_1 = C_2$ in equation (2.19):

$$G_1(\omega) = -G_2(\omega) = \frac{1}{2}\{\alpha_1(g_{11} - g_{21}) + \alpha_2(g_{22} - g_{12})\}. \tag{3.2}$$

In section 4, we will numerically compare our results obtained from equation (2.19) to those obtained from equation (3.2).

4. Numerical examples

In this section, we demonstrate the effect of charging on the ac conductance by comparing the conductances calculated with and without charging. The values of ϵ_r, Γ_1 and Γ_2 are chosen only to illustrate the discussion of section 3. Capacitances comparable to those used here are possible only in devices with very narrow cross sections. The discussion of section 3 is however valid for broad-area resonant tunnelling devices as well, where the effect of capacitances is equally important. In example 1, we start with a device which is symmetric both in the barrier strengths and capacitances, at zero bias. Here the conductances calculated from equations (2.19) and (3.2) are comparable. The effect of introducing an asymmetry in

only the barriers (example 2) and the capacitances (example 3) of the structure in example 1 is then studied. In example 4, we discuss the ac conductance of a device in the presence of an applied bias. In the numerical examples considered here, we have verified that the low-frequency ac conductance is equal to the differential conductance of the dc I–V curve.

4.1. Example 1. A symmetric device at zero bias

The conductance versus frequency with and without charging (equations (2.19) and (3.2)) are found to be the same (the circles and crosses of figure 3). This is because in the special limit of a symmetric device at zero bias, the ac charge density in the well is zero (This follows from equations (2.10), (2.12), (2.13) and by noting that, for a symmetric structure at zero bias, $g_{ij} = g_{ji}$.) As a result, both the ac potential and the displacement currents due to the charge in the well are zero. The parameters chosen in this example are: $V_{dc} = 0$ V, the chemical potential of contact 1 (μ_1) and contact 2 (μ_2) are chosen to be 10 meV, $\epsilon_r = 10$ meV, $\Gamma_1 = \Gamma_2 = 0.1$ meV at $E = \epsilon_r$, $w = 2000$ meV, $w_1 = w_2 = w/16.7$, $C_1 = C_2 = 2 \times 10^{-16}$ F and $kT = 0.015$ meV.

4.2. Example 2. The effect of asymmetry only in the barrier strength

The structure is identical to that in example 1 except that the barriers are asymmetric ($\Gamma_1 = 0.02$ meV and $\Gamma_2 = 0.1$ meV). Then, the results predicted by equations (2.19) and (3.2) are comparable (figure 2(a)). This can be explained as the total capacitance between the device and the contacts is so large that the contribution to the ac potential in the well due to the $q(\omega)/C$ term in equation (2.3) is negligible and that $C_1 = C_2$ (see the discussion in section 3).

When there is an asymmetry in the capacitances, charging should always be included properly.

In the case of a structure with smaller capacitances ($C_1 = C_2 = 1 \times 10^{-16}$ F), the results obtained from equations (2.19) and (3.2) are different (figure 2(b)). This is because when the total capacitance is small, the potential of the well is altered significantly by the charge in it. Then, the conduction currents calculated with and without charging included are different. Note that equation (3.2) does not predict a change in the ac conductance when the capacitances are changed without altering the ratios α_1 and α_2 (see the circles and crosses in figures 3(a) and 3(b)).

4.3. Example 3. The effect of asymmetry only in the capacitances

A DBRTS for which an asymmetry in the capacitances has been introduced in example 1 ($C_1 = 1 \times 10^{-15}$ F and $C_2 = 5 \times 10^{-15}$ F; the barriers are symmetric) is now considered. Here C is large enough that the q/C term does not contribute substantially to the ac potential in the well. The results obtained from equations (2.19) and (3.2) are different (figure 3) because unequal displacement currents flow in the two contacts when $C_1 \neq C_2$. Then, a simple averaging of the conduction currents as in equations (3.1) and (3.2) is no longer valid. Note that the result for the ac conductance from equation (3.2) is identical in examples 1 and 3 because equation (3.2) does not correctly account for the asymmetry in the capacitances.

4.4. Example 4. ac conductance in the presence of an applied voltage

The dc bias is chosen to be $V = 5$ mV for the example in figure 4 and the self-consistently determined position of the resonance is 10.5362 meV. The values of the various parameters

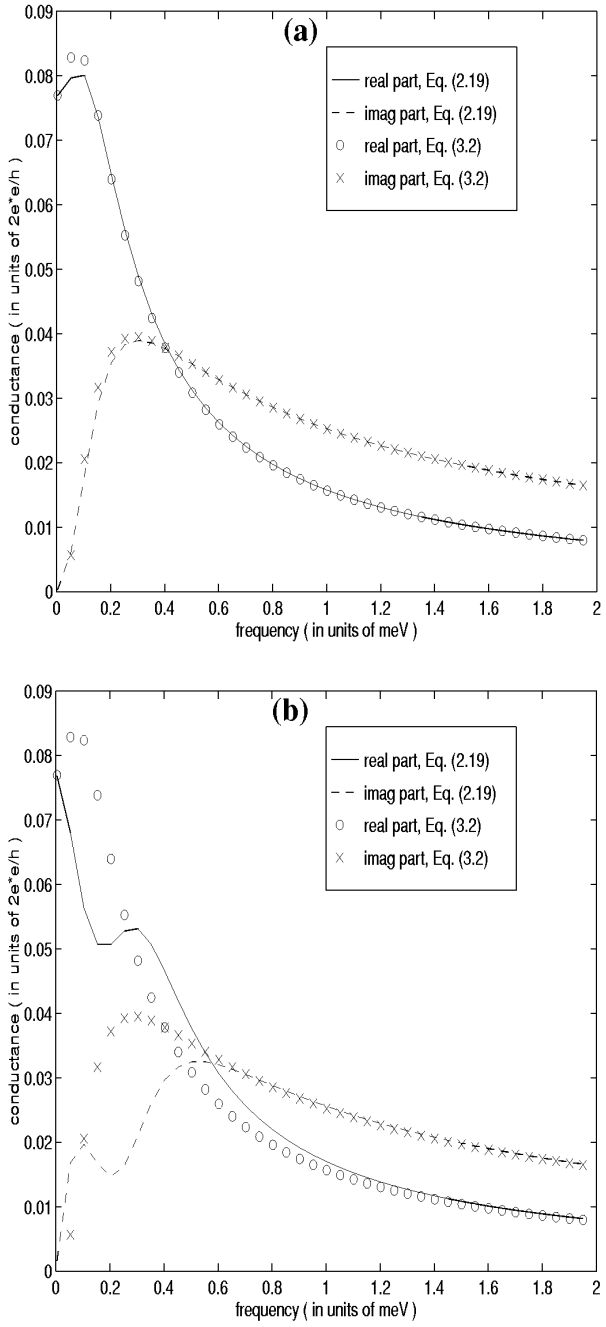

Figure 2. *Asymmetry just in the barrier strengths.* (a) For a structure in which the only asymmetry is in the barrier strength, neglecting charging is a good approximation when the total capacitance between the well and the contacts is large. (b) For the same structure as in (a), neglecting charging is not a reasonable approximation when the total capacitance between the well and the contacts is small.

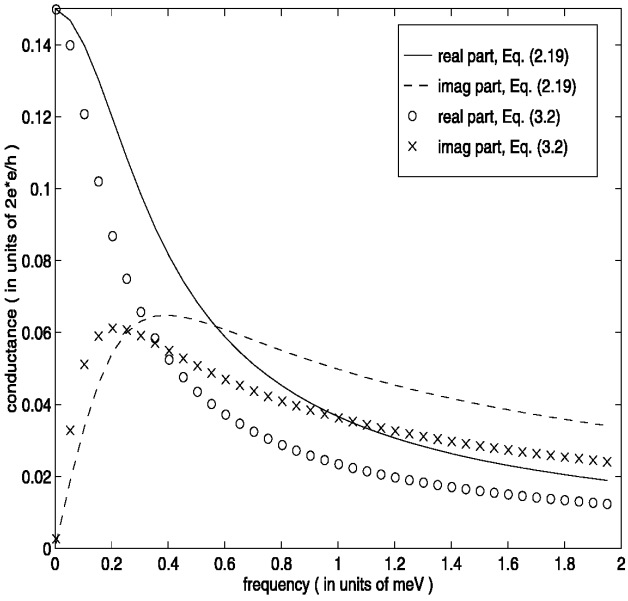

Figure 3. *Asymmetry just in the capacitances.*

are $C_1 = C_2 = 1 \times 10^{-15}$ F, $w = 2000$ meV, $w_1 = w/17.1$, $w_2 = E/17.1$, $\epsilon_{r0} = 8.0$ meV, $\mu_1 = 15$ meV, $\mu_2 = 10$ meV and $kT = 0.037$ meV. From figure 4(a), we see that the elements of the g-matrix, g_{12} and g_{22}, are larger than g_{21} and g_{11} respectively. This feature can be understood by noting that the g-matrix elements depend on the variation of the Fermi function in the contacts and that this variation is more rapid around the resonant energy in contact 2 than in contact 1 (equation (2.29)). Also, the real part of g_{12} and the imaginary part of g_{22} exhibit a peak around a frequency of 0.5 meV because the resonant energy in the well is about 0.5362 meV above the chemical potential of contact 2. We are in the regime where the q/C component of V_w is negligible and $C_1 = C_2$. So the ac conductance here agrees well with that obtained from equation (3.2). From equation (2.19), we find that

$$G_1(\omega) = \frac{1}{4}(g_{11} + g_{22} - g_{12} - g_{21}).$$

This expression explains why the ac conductance looks similar to g_{22}, the largest of the g-matrix elements (figure 4(b)).

On the other hand, we know from section 3 that for a device where $C_1 \neq C_2$, the ac conductance depends on the ratio of C_1 and C_2. To illustrate this, we keep the values of the resonant energy, applied bias and all other parameters the same as those used in figure 4(b), except that $C_2 = 4 \times C_1 = 4 \times 10^{-15}$ F. From equation (2.19),

$$G_1(\omega) = \frac{16}{25}g_{11} + \frac{1}{25}g_{22} - \frac{4}{25}(g_{12} + g_{21}).$$

While the g-matrix elements remain the same as in figure 4, it is obvious from the expression for $G_1(\omega)$ that the conductance here is very different from that in the previous case (figure 4(c)). In contrast, equation (3.2) predicts the same value for the ac conductance in the two cases [19].

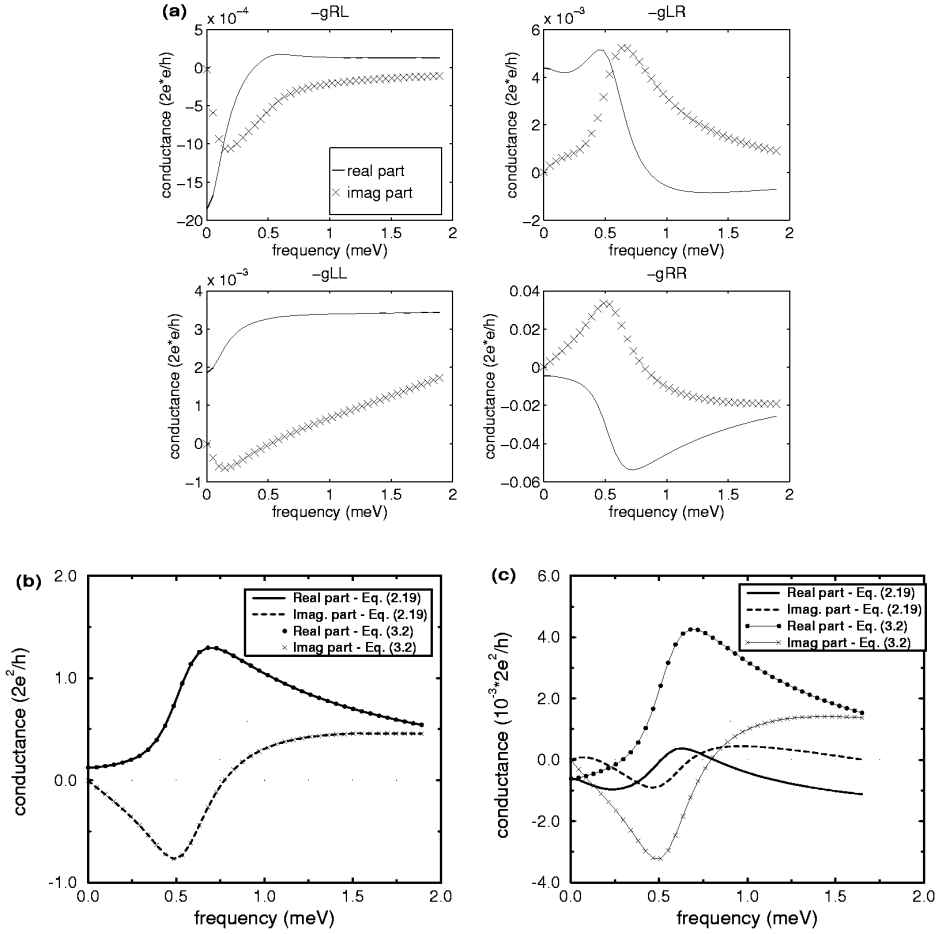

Figure 4. *ac conductance in the presence of an applied bias.* (a) The conductance matrix elements. (b) The total conductance looks similar to the largest conductance matrix element g_{22} for this structure when $C_1 = C_2$. (c) The total conductance for a device for which $C_2 = 4C_1$ is, however, different from case (b).

4.5. Experiments

We now make some remarks on the experimental conditions necessary to observe the differences in the ac conductance discussed. Example 1 corresponds to a symmetric GaAs–AlGaAs structure with identical barriers on either side. A structure with equal capacitances between the well and the two contacts but with different coupling strengths to the contacts (example 2) can be constructed as follows. The coupling across the left-hand barrier can be made weaker by increasing the barrier height. For AlGaAs, the dielectric constant does not change significantly as the Al doping is increased in the left-hand barrier so as to increase the barrier height. As a result, the barriers will have nearly the same widths and hence capacitances. With regards to example 3, the capacitance across the second barrier can be made five times larger by making the barrier about five times thinner than the first barrier. To have similar transmission coefficients, the barrier height of the second barrier should be correspondingly increased. These requirements can probably be met with the present

advances in band-gap engineering and the exact values of the barrier heights and widths are easy to determine. What is more difficult to achieve is the close proximity of the contacts to the barriers that we have assumed in this paper. This assumption was however made only to make the calculations simpler, and more realistic calculations that are beyond the scope of the present work can be carried out.

5. Conclusions

In this paper, we have calculated the ac conductance of a DBRTS by including the effect of imaging of charge from the well to the two contacts and present useful expressions to calculate the ac conductance of a DBRTS. The formalism is applicable at high frequencies and in the presence of finite dc biases. The self-consistent inclusion of the effect of imaging of well charge is central to calculating total currents which are equal in the two contacts. We find that including the effect of imaging of charge from the well to the contacts plays a significant role in determining the ac conductance of a DBRTS. The time-varying charge density in the well contributes to a flow of displacement currents equal to

$$\frac{C_1}{C}\frac{\mathrm{d}q}{\mathrm{d}t} \qquad \text{and} \qquad \frac{C_2}{C}\frac{\mathrm{d}q}{\mathrm{d}t}$$

in contacts 1 and 2 respectively ($q(t)$ is the well charge). The strength of imaging which is modelled by the total capacitance C plays a role in determining the ac potential in the well via the $q(t)/C$ term. These features were illustrated using simple numerical examples in section 4. Some previous papers calculated the ac conductance of a DBRTS by the following procedure. The conduction currents across the two barriers were calculated by neglecting the contribution to the ac potential in the well due to imaging of the time-dependent charge density. Then the total ac current was taken to be the average of the conduction currents flowing across the two barriers. In conclusion, we have shown that such a procedure for calculating the ac conductance is correct only when both the capacitance is symmetrical ($C_1 = C_2$) and the value of C is large.

Acknowledgments

I would like to thank Supriyo Datta for discussions on various aspects of transport in mesoscopic systems and David Janes for discussions pertaining to the experimental feasibility of some of the results of the paper. Part of this work was carried out at Purdue University and financial support through NSF grant number ECS-9201446-01 (Supriyo Datta) is acknowledged.

References

[1] Buot F A 1993 *Phys. Rep.* **234** 73 (see section 4)
[2] Frensley W R 1988 *Superlatt. Microstruct.* **4** 497
[3] Buot F A and Rajagopal A K 1993 *Phys. Rev.* B **48** 17 217
[4] Jacoboni C and Price P J 1990 *Solid State Commun.* **75** 193
[5] Liu H C 1991 *Phys. Rev.* B **43** 12 538
[6] Chen L Y and Ting C S 1990 *Phys. Rev. Lett.* **64** 3159
[7] Fu Y and Dudley S C 1993 *Phys. Rev. Lett.* **70** 65
[8] Landauer R 1992 *Phys. Scr.* T **42** 110
[9] Büttiker M, Pretre A and Thomas H 1993 *Phys. Rev. Lett.* **70** 4114
[10] Büttiker M, Thomas H and Pretre A 1993 *Phys. Lett.* **180A** 364
[11] Büttiker M 1993 *J. Phys.: Condens. Matter* **5** 9361

[12] Anantram M P and Datta S 1994 *Phys. Rev.* B **51** 7632
[13] Christen T and Büttiker M 1996 *Phys. Rev.* B **53** 2064
This reference includes the important effect of dephasing in the ac conductance using voltage probes.
[14] Sheard F W and Toombs G A 1988 *Appl. Phys. Lett.* **52** 1228
[15] Datta S 1995 *Electronic Transport in Mesoscopic Systems* (Cambridge: Cambridge University Press)
[16] From equations (2.3) and (2.5)), $v_w(t) = v_w^{ac}(t) + \alpha_2 v_1^{ac}(t)$.
[17] Mahan G D 1991 *Many Particle Physics* 2nd edn (New York: Plenum)
[18] Lake R, Klimeck G and Datta S 1993 *Phys. Rev.* B **47** 6427
[19] The position of the resonance is not calculated self-consistently here, as we only want to illustrate the effect of changing the capacitances.